University of Sheffield

Department of Control Engineering

An adaptive analogue tracker for automatic measurement of time-varying lung parameters

M. D. Nada and D. A. Linkens

Research Report No. 38

January 1976

An adaptive analogue tracker for automatic measurement of time-varying lung parameters.

M. D. Nada D. A. Linkens

ABSTRACT

This research report describes the design and results obtained using simple electronic circuits specially designed for implementing a simple lung parameter tracking algorithm for identification of the mechanical properties of the lung. Unlike the commonly used loop-flattening technique, the adaptive electronic tracker is able to monitor continuously the mechanical properties of the respiratory system. It is capable of tracking the rapid changes in lung parameters as the frequency of breathing changes. The design of the adaptive tracker is based on equation-error formulation and the global asymptotic stability of the adaptive tracking equations is guaranteed. The cheapness and simplicity of the tracker makes it suitable for clinical applications.

Nomenclature

P_m	mouth pressure
P_p	intrapleural pressure
P_o	intraoesophageal pressure
V	lung volume
$\dot{V}$	airflow into the lungs
R	lung resistance
E	lung elastance
R_s, E_s	scaled parameters proportional to R, E
$\hat{R}_s$, $\hat{E}_s$	estimates of R_s, E_s
$\acute{P}$, $\acute{\dot{V}}$, $\acute{V}$	filtered versions of P, $\dot{V}$, V signals
ε	error signal in parameter tracking system

1. Introduction

This research report describes simulation and experimental studies in identification of lung parameters. The lung should be modelled as a complex distributed parameter system. To characterize the lungs simply, however, a mathematical model with two unknown parameters is extensively used in clinical applications. These two parameters represent the resistance of the airways and lung tissues, and the elastance of the lung and chest wall. Because of the simplicity of the problem it was decided to avoid the complexity of a digital algorithm using a Kalman-Bucy filter [1] or the method of recursive least squares. Instead a suboptimal analogue solution based on a steepest descent gradient algorithm[2,11]was implemented.

1.1 Mathematical lung model

A simple mathematical model for the lung, relating inspired airflow, lung volume, and pressure is extensively used in clinical applications [5] and is described by

$$P_m - P_p = R\dot{V} + EV \qquad (1)$$

where,

P_m = mouth pressure (cm H_2O)

P_p = intrapleural pressure (cm H_2O)

R = resistance of airways and lung tissue (cm H_2O sec/litre)

E = elastance of the lung and chest wall (cm H_2O/litre)

$\dot{V}$ = airflow into the lungs (litre/sec)

V = lung volume (litres)

In order to determine the lung parameters R and E it is clear that P_m, P_p, $\dot{V}$ and V must be measured. Clinically the measurement of intrapleural pressure is difficult and dangerous and normally the intraoesophageal pressure P_o is measured [4]. Unfortunately, the measurement of this pressure is always corrupted with noise due to peristalsis waves and contractions of the heart [4,5].

A further factor is that the airflow through the variable geometry mucus-lined airways is partly laminar and partly turbulent [3,6]. The elastic energy term of equation (1) has both plastoelastic and linear viscoelastic components [7]. In general, the limitations of the mathematical lung model can be summarised as follows;

(1) This model is poor during forced expiration of normal subjects and during normal expiration of subjects suffering from chronic obstructive lung disorders such as bronchitis and emphysema.

(2) This model is poor when the airflow is high because the flow is then turbulent and it is more accurate to model the resistive term as,

$$R = R_1 + R_2 |\dot{V}| \tag{2}$$

where R_2 is a resistive term to account for turbulent flow.

This modelling error usually affects the estimation of the lung parameters as it can lead to biased estimates of the resistance and elastance.

1.2 Signal Conditioning

During clinical artificial ventilation the signals that can be measured are P_m, P_o and $\dot{V}$, but lung volume is generally inaccessible. However, a good estimate of the lung volume can be obtained by direct integration of the airflow $\dot{V}$. Due to the limitations in the lung model mentioned in the previous section, the parameters were estimated using inspiratory data alone, which gives a better fit to equation (1). Drift problems in integrating the airflow $\dot{V}$ were also overcome by using an integrate/reset amplifier which was reset during expiration. The pressure, flow and volume signals must be modified so that equation (1) is satisfied at the starting time of inspiration ($t = t_o$, $V(t_o) = 0$). Thus, the following filtered values of the signals P, $\dot{V}$ and V which represent the pressure, flow and lung volume respectively are obtained;

$$\begin{aligned} \acute{P}(t) &= K_p((P_m(t) - P_o(t)) - (P_m(t_o) - P_o(t_o))) \\ \acute{\dot{V}}(t) &= K_{\dot{V}}(\dot{V}(t) - \dot{V}(t_o)) \\ \acute{V}(t) &= K_V \int \acute{\dot{V}}(t)\, dt \end{aligned} \tag{3}$$

where,

K_p = gain of the preamplifier and pressure transducer (volt/cm H_2O)

$K_{\dot{V}}$ = gain of the preamplifier and flow transducer (volt.sec/litre)

K_V = gain of the lung volume integrate/reset amplifier (sec^{-1})

Equation (1) thus becomes

$$\acute{P}(t) = R_s \acute{\dot{V}}(t) + E_s \acute{V}(t) \tag{4}$$

where R_s and E_s are scaled values of the actual lung parameters and can be written as

$$\left.\begin{aligned} R_s &= \frac{RK_p}{K_{\dot{V}}} \\ E_s &= \frac{EK_p}{K_V K_{\dot{V}}} \end{aligned}\right\} \tag{5}$$

2. LUNG PARAMETERS IDENTIFICATION

The lung parameters may be estimated directly without observing lung volume V(t) using a model reference system based on the response-error formulation (Figure 1), but this solution is non-linear [2]. In this case the model parameters α_i are adjusted according to a steepest descent law

$$\dot{\alpha}_i = -K \frac{\partial F}{\partial \alpha_i} \tag{6}$$

where F is a performance criterion which is a quadratic function of the response-error and K is the adaptive gain. The response error system has the advantage that only the system input and output need to be measured. The steepest descent path followed in the parameter space is, however, only an approximation. The equation-error on the other hand is an algebraic function of the parameters, hence the partial derivative in (6) is truly defined and a steepest descent path in parameters space is accurately followed. In equation-error systems, however, all state variables must be measured or generated [8]. For the design presented in this research report an equation-error formulation which required previous estimation of lung volume V(t) was chosen due to its simplicity of implementation. The parameters were estimated using inspiratory data alone and the lung volume V(t) was obtained by integration of airflow $\dot{V}(t)$.

2.1 Lung parameters adjustment laws

Using estimates $\hat{R}_s$, $\hat{E}_s$ of R_s and E_s an estimation-error equation is generated as,

$$\varepsilon = \acute{P} - \hat{R}_s \acute{\dot{V}} - \hat{E}_s \acute{V} \qquad (7)$$

Hence, from equation (4) we get

$$\varepsilon = \acute{\dot{V}}(R_s - \hat{R}_s) + \acute{V}(E_s - \hat{E}_s) \qquad (8)$$

giving

$$\varepsilon = \acute{\dot{V}}\tilde{R}_s + \acute{V}\,\tilde{E}_s \qquad (9)$$

where,

$\tilde{R}_s = (R_s - \hat{R}_s)$ is the instantaneous deviation in tracking R_s

and $\tilde{E}_s = (E_s - \hat{E}_s)$ is the instantaneous deviation in tracking E_s

Equation (9) can be written in vector form as

$$\varepsilon = \underline{\Theta}.\underline{\tilde{X}} \qquad (10)$$

where, $\underline{\tilde{X}}^T = (\tilde{R}_s \;\; \tilde{E}_s)$

and $\underline{\Theta} = (\acute{\dot{V}} \;\; \acute{V})$, $\underline{\tilde{X}} = \underline{X} - \underline{\hat{X}}$

The parameters adjustment law can be written as

$$\frac{d}{dt}[\underline{\hat{X}}] = - M . \frac{\partial}{\partial \hat{X}} F(\varepsilon) \qquad (11)$$

where $F(\varepsilon)$ is the error performance criterion which is chosen here to be

$$F(\varepsilon) = \tfrac{1}{2}.\varepsilon^2 \qquad (12)$$

and [M] is [2 x 2] positive definite diagonal matrix defined as the gain matrix, hence using (10) one obtains

$$\frac{d\hat{\underline{X}}}{dt} = M\underline{\Theta}^T \cdot \frac{\partial F(\varepsilon)}{\partial \varepsilon} \qquad (13)$$

giving

$$\begin{bmatrix} \dot{\hat{R}}_s \\ \dot{\hat{E}}_s \end{bmatrix} = \begin{bmatrix} m_1 & 0 \\ 0 & m_2 \end{bmatrix} \cdot \begin{bmatrix} \acute{\hat{V}} \\ \acute{V} \end{bmatrix} \cdot \varepsilon \qquad (14)$$

Using the following substitutions

$$x_1 = R_s / \sqrt{m_1} \;,\quad x_2 = E_s / \sqrt{m_2} \;,\quad \hat{x}_1 = \hat{R}_s / \sqrt{m_1} \;,\quad \hat{x}_2 = \hat{E}_s / \sqrt{m_2},$$

$$h_1 = \acute{\hat{V}} \sqrt{m_1} \;,\quad h_2 = \acute{V} \sqrt{m_2} \;,\quad \tilde{x}_i = x_i - \hat{x}_i \;;\quad i = 1,2$$

equation (9) becomes,

$$\varepsilon = h_1 \tilde{x}_1 + h_2 \tilde{x}_2 \qquad (15)$$

and equation (14) becomes,

$$\begin{bmatrix} \dot{\hat{x}}_1 \\ \dot{\hat{x}}_2 \end{bmatrix} = \begin{bmatrix} h_1 \\ h_2 \end{bmatrix} \cdot \varepsilon \qquad (16)$$

which can be written in vector form as

$$\dot{\hat{\underline{x}}} = \underline{H}^T \cdot \varepsilon \qquad (17)$$

where

$\dot{\hat{\underline{x}}}$ = (2 x 1) Column vector ,

$\underline{H}^T$ = (2 x 1) Column vector

and using the parameter misalignment vector ($\tilde{\underline{x}} = \underline{x} - \hat{\underline{x}}$) equation (17) can be rewritten as

$$\dot{\tilde{\underline{x}}} = -\underline{H}^T \cdot \varepsilon + \dot{\underline{x}} \qquad (18)$$

2.2 Stability analysis of the parameters adjustment laws

The system described by equation (18) is asymptotically stable in the large and hence the null solution $\hat{\underline{x}}=0$ is an asymptotically stable equilibrium point in the parameters deviation plane. This can be proved as follows, choosing a Lyapunov function

$$V(\hat{\underline{x}}) = \tfrac{1}{2}\,\hat{\underline{x}}^T \cdot \hat{\underline{x}} = \tfrac{1}{2}(\hat{x}_1^2 + \hat{x}_2^2) \tag{19}$$

which has a derivative

$$\begin{aligned}\dot{V}(\hat{\underline{x}}) &= -(\hat{\underline{x}}^T \cdot \underline{H}^T) \cdot (\underline{H} \cdot \hat{\underline{x}}) \\ &= -\varepsilon^2\end{aligned} \tag{20}$$

hence $\dot{V}(\hat{\underline{x}})$ is negative semi-definite and the system is stable. Now, if $\dot{V}(\hat{\underline{x}}) = 0$ then either $\hat{\underline{x}} = \underline{0}$ continuously which is the desired equilibrium point or $\underline{H}.\hat{\underline{x}} = 0$ continuously and $\dot{\hat{\underline{x}}} = \underline{0}$. It is not possible, however, to find an $\hat{\underline{x}}$ which satisfies $\underline{H}.\hat{\underline{x}} = 0$ continuously unless $\underline{H}$ and $\hat{\underline{x}}$ are orthogonal. Therefore, the system described by equation (18) is asymptotically stable provided $\underline{H}$ and $\hat{\underline{x}}$ are not orthogonal. From equation (19) it is clear that $V(\hat{\underline{x}}) < \infty$ if $\|\hat{\underline{x}}\| < \infty$ and $V(\hat{\underline{x}}) \to \infty$ as $\|\hat{\underline{x}}\| \to \infty$ hence the null solution $\hat{\underline{x}} = \underline{0}$ is asymptotically stable in the large [9].

3. ANALOGUE ADAPTIVE TRACKER

3.1 Electronic design of the tracker

The tracker was built using available cheap components and it consists of three main parts.

Part (1)

Preamplifiers and filtering stage which consists of buffers, variable-gain amplifiers, second-order Butterworth low-pass filters with cut-off frequency 5.0 Hz [10], overload and under-load indicators. Figure (2) shows the circuit diagram of this section, while Figure (3) shows details of the peak detector and load indicators. An additional peak detector and load indicator is also included on this board for the volume signal.

Part (2)

Signal conditioning stage for generating the signals given by equation (3). It consists of a compute-reset integrator, a track-hold amplifier, a compute-reset amplifier and zero-crossing comparator with exponentially decaying hysteresis. Figure (4) is the circuit diagram of this second section.

Part (3)

The adaptive circuit which consists of two compute-hold integrators, four internally-trimmed linear multipliers, and a summer amplifier. Two ten-turn 10 KΩ variable coefficient potentiometers are used to set the values of the adaptive gains m_1 and m_2. Figure (5) shows the circuit diagram of this section.

General notes on the design are as follows:

(1) The current requirement of the circuit is 50 mA from -15, 0, +15V power supplies. A regulated dc supply is highly desirable.

(2) Metal oxide resistors 1.0% tolerance, $\frac{1}{2}$ watt were used in the circuit to maintain the required accuracy. Single asterisks in the circuit diagram denote specially matched components which are used in the design of the compute-reset integrator, track-hold amplifier, and compute-hold integrator.

(3) All multipliers are type AD532JD, internally trimmed with full scale error ± 1.0 % and percentage harmonic multiplication nonlinearity between ± 0.3 and ± 0.8%. The input pins were chosen to minimise feedthrough and multiplication nonlinearity.

(4) The track-hold amplifier, compute-reset integrator and compute-hold integrators are all type LM312 super gain amplifiers.

(5) All electronic switches used are MOS transistors type ML101B.

(6) Two moving coil dc meters were fitted on the front panel for direct measurement of the estimated parameters R, E and for testing all signals through the circuit.

3.2 <u>Tests on simulated data</u>

The accuracy and dynamic response of the tracker was first investigated using sinusoidal inputs.

(a) Accuracy

The tracker was tested using sinusoidal signals in the frequency range 0.3 - 1.0 Hz which is close to normal breathing frequencies. Equation (1) was simulated on a small analogue computer (Vidac 336 - Computing Techniques Ltd.)

using a summer amplifier and 2 ten-turn, 10 K variable coefficient potentiometers. The potentiometers settings were adjusted to represent the value of the parameters R and E. For various settings of R and E and in a frequency range 0.3 - 1.0 Hz the tracker was thoroughly tested and it was found that it estimated the parameters successfully with typical accuracy of better than 2.0%. Tables (1) (2) show estimated values of R and E for different preset values on the analogue computer. These tables show a worst-case error in estimating R of 1.4% and 1.6% in estimating E.

(b) Dynamic Response

The time responses of the tracker in the frequency range 0.3 - 1.0 Hz for adaptive step changes were recorded. They showed that for the appropriate adaptive gain settings m_1, m_2 the tracker was always able to track the exact parameters within two cycles of the input signal figure (6a, b and c).

Table (3) shows the convergence time and the corresponding adaptive gain settings for the parameters R and E to settle within 5% of their steady-state values. This table shows that the convergence time varies as the frequency of the input signal varies and also that it depends on the adaptive gain settings. No instability problems were found for the adaptive gains used.

(c) Tracking slowly time-varying parameters

The parameters R and E in equation (1) were now assumed to be time-varying. Setting R and E to slowly ramp functions given by, $R(t) = a_1t$ and $E(t) = a_2t$, the dynamic response of the tracker was investigated. Figures (7a, b and c) show typical recordings. The error in estimating R(t) and E(t) decreased as the slope of the ramp was decreased and as the frequency of the input signal was increased. R and E in equation (1) were also simulated by slowly-varying sinusoids given by

$$R(t) = A \sin 2\pi f_1 t$$

$$E(t) = A \cos 2\pi f_1 t$$

and the tracker dynamic response was obtained. Figures (8a, b and c) show the parameters $\hat{R}(t)$ and $\hat{E}(t)$ for different frequencies of the input signal ($\dot{V}$ in equation (1)). These recordings show that the dynamic response was improved and the error in estimating the parameters R(t) and E(t) decreased, if these parameters were varying slowly enough with respect to the rate of adjustment of these parameters. The parameter adjustment law given by equation (14) dominates the rate of adjustment of these parameters. It was also noticed that better performance of the tracker was achieved if the frequency of the input signal was increased.

It should be noticed that the ability of the tracker to track time-varying parameters is limited to slowly time-varying parameters. For fast variation in parameters, instability problems would arise and the adjustment law given by equation (14) is no longer valid.

4. EXPERIMENTAL STUDIES

4.1 Method

Having tested the electronic tracker on simulated data it was used in clinical studies for estimating the mechanical properties of the respiratory system. The oesophageal balloon technique [4] was used to measure the intraoesophageal pressure of a conscious healthy sitting subject. A thin latex balloon (10 cms length, 0.7 cms diameter) sealed over ten spirally arranged perforations made at the end of a thin polyethylene catheter (inside diameter = 0.9 mms, outside diameter 2.0 mms and length = 100 cms) was used for recording the intraoesophageal pressure. The tip of the balloon was positioned to approximately about 40 cms from the nostril holes and 5.0 cms above the cardiac sphincter to avoid heart contractions. The volume of the balloon was adjusted to 0.5 cm^3. The flow signal was measured using a calibrated A. Fleish pneumotachograph having a dead space of 60 cm^3 and a resistive element of coil corrugated foil with resistance = 0.40 cm H_2O.sec./litre. A 6 volt dc supply was used to heat the resistive element to prevent vapour condensation on it. A differential pressure transducer type U.P. (range $\pm$ 25.6 cms W.G.) was used for sensing the pressure drop across the resistive element together with a Cambridge pressure channel type 01079

(Cambridge Medical Instruments).

The differential pressure from the mouth and the oesophagus was sensed using a differential pressure transducer type U.P. (range $\pm$ 25.6 cms W.G.) with the same Cambridge pressure channel.

The pressure and flow signals were recorded while the subject was sitting during normal breathing (frequency $\approx$ 0.3 – 0.6 Hz) and panting (frequency $\approx$ 1.0 – 1.5 Hz).

4.2 Results

Figures (9a,b) and (10) show the tracker estimates of R_s and E_s during normal and fast breathing respectively. Figure (11) shows the fast response of the tracker as the frequency of breathing was increased. The values of K_p, $K_{\dot{V}}$ and K_V in equation (3) were chosen as 5.45 volt/cm H_2O, 1.97 volt.sec/litre, and 3.07 second^{-1} respectively. The meter range factor in Figure (5) was equal to 0.3. An increase in the frequency of breathing caused the elastance to increase which agrees with the previous reports [7,12]. The airways resistance was found to be varying due to the increase of airflow velocity which would tend to increase the Reynold's number of flow through the airways. However, due to the fact that only inspiratory data was being used the changes in the airway resistance were generally small. Table (4) gives estimates of R and E at different breathing frequencies. The tracker estimates were compared with values obtained from the loop-flattening method. In this method the signal $Y = P - \hat{E}V$ is generated electronically, where $\hat{E}$ is a manually adjustable variable (signals P and V being the pressure and volume respectively). The signal Y is displayed on the Y axis of an X-Y plotter or oscilloscope, and a signal proportional to $\dot{V}$ is displayed on the X-axis. If the measurements satisfy equation (1), then for repetitive breathing waveforms, the resulting closed loop may be reduced to a straight line of slope proportional to $\hat{R}$ by manually adjusting $\hat{E}$ until $\hat{E} = E$. If the resistive pressure drop in (1) is a non-linear function of $\dot{V}$ then the loop may be reduced to a curved line. If both the resistive and elastic terms are non-linear, then exact loop flattening is impossible. Using this method, the data obtained as described in 4.1 was analysed. A number of loops were flattened during three different stretches of normal breathing. Three flattened loops were selected and five photocopies were obtained for each loop. The average slope was calculated for the five photocopies together with the corresponding standard deviation. Table (5) gives estimates of R and E using loop-flattening technique for the three loops and the corresponding values of the estimates at the same instants (indicated by arrows in Figure (9a,b)) using the adaptive tracker. The loop-flattening technique was difficult to apply to panting data whereas the tracker behaved normally.

The maximum standard deviation in estimating the average slope was 0.118 and this is equivalent to approximately 7° of slope and thus the percentage error in estimating the loop slope was about $\pm 10\%$.

CONCLUSION

The electronic design of an adaptive tracking algorithm for identifying the lung parameters has been described. The pressure and flow signals were filtered and conditioned to give only inspiratory data using a track-hold circuit for the pressure signal and a compute-reset amplifier for the flow signal. The volume signal was estimated using an integrate-reset amplifier and thus drift problems in integration were avoided. The inspiratory data alone was used for estimating the mechanical properties of the lung since these pressure, flow and volume signals fit equation (1) more accurately than for expiratory data. The adaptive tracker was first tested using sinusoidal signals for which it was found that it had a maximum percentage error in estimation of less than $\pm 2.0\%$.

In terms of dynamic response it was able to track the exact parameters within a few cycles of breathing (typically less than 2).

Results obtained during clinical studies showed that as the frequency of breathing changed the lung elastance was changed. These results agreed with the previous results reported by other investigators. Results obtained by the loop-flattening technique and compared with those obtained using the adaptive tracker showed that the tracking algorithm was a good estimator for the lung parameters, and that it has a better accuracy than the loop-flattening technique. It also had the facility of tracking the parameters continuously and was able to recover very quickly especially if the pressure signal was affected by heart contractions or peristalsis.

Any method for monitoring physiological parameters which does not relate directly to the survival of the patient is unlikely to find wide clinical acceptance unless it is relatively cheap. For this reason, simplicity and cheapness were prime considerations in the present design. All components and elements used in the design were chosen from available cheap commercial components and the resultant tracker design has shown the feasibility of obtaining high accuracy, fast estimates of lung parameters at low cost.

ACKNOWLEDGEMENTS

The authors are greatly indebted to Dr. M. L. Bransby, former lecturer in the Department of Control Engineering, Sheffield University, and staff of the Medical Physics Department at the Weston Park Hospital, and also staff of the Breathing Test Laboratory at the Royal Hospital, Sheffield, England, for their valuable assistance in conducting the clinical experiments. The assistance and encouragement of Dr. M. L. Bransby during the initial progress of this research is greatly acknowledged.

REFERENCES

(1) Kalman, R. E. and Bucy, R. S.
"New results in linear filtering and prediction theory", Trans. ASME ser. D. J. Basic Engng., 1961, 83, 95-108.

(2) Lion, P. M.
Rapid identification of linear and nonlinear systems, AIAA Journal, 1967, 5, 1835-1842.

(3) Olson, D. E. et al.
"Pressure drop and fluid flow regime of air inspired into the human lungs", J. Appl. Physiology, 28, 1970, 482-494.

(4) Mead, J. et al.
"Measurement of intraoesophageal pressure", Journal of Applied Physiology, 7, 491-495, 1955.

(5) Cotes, J. E.
Lung function - assessment and application in medicine, Blackwell Scientific Publications, 3rd edition, 1975.

(6) Fry, D. L.
"A preliminary lung model for simulating the aerodynamics of the bronchial tree", Computers and Biomedical Research 2, 111-134, 1968.

(7) Hildebrandt, J.
"Pressure - volume data of cat lung interpreted by a plastoelastic - linear viscoelastic model", Journal of Applied Physiology, 28, 1970, 365-372.

(8) Mendel, J. M.
"Gradient estimation algorithm for equation error formulations", IEEE Trans. on Automatic Control, Vol. AC-19, No. 6, 1974, 820-824.

(9) La Salle, J. and Lefschetz, S.
"Stability by Lyapunov's direct method with applications", New York, Academic Press, 1961.

(10) Operational amplifiers - design and applications.
McGraw-Hill Book Company Inc. 1971.

Editors: Tabey, G. E., Graeme, J. G. and Huelsman, L. P.

(11) Bransby, M. L. and Nightingale, J. M., "Lung Parameters Tracking", 6th World Congress, Boston, U.S.A., 1975.

(12) Otis, A. B. et al., "Mechanical factors in distribution of pulmonary ventilation", Journal of Applied Physiology, 8, 1956, 427-443.

FIGURE CAPTIONS

Figure 1 Block diagram of equation-error and response-error identification systems.

Figure 2 Circuit diagram of board containing buffers, inverters, low-pass filters, variable gain amplifiers.

Figure 3 Circuit diagram for peak detector and load indicator.

Figure 4 Circuit diagram of board containing signal conditioning stages.

Figure 5 Circuit diagram of adaptive tracking section.

Figure 6 Dynamic response of tracker using simulated data.

(a) input frequency = 1.0 Hz, adaptive gain = 0.6

(b) " " = 0.6 Hz, " " = 0.6

(c) " " = 0.3 Hz, " " = 0.8

Figure 7 Tracking slowly time-varying parameters R(t) = 0.5t, E(t) = 0.5t.

(a) Input frequency = 0.3 Hz

(b) " " = 0.6 Hz

(c) " " = 1.0 Hz

Figure 8 Tracking slowly varying sinusoidal parameters R(t) = 2.0 sin 0.5t, E(t) = 2.0 cos 0.5t.

(a) input frequency = 0.3 Hz

(b) " " = 0.6 Hz

(c) " " = 1.0 Hz

Figure 9a,b Response of tracker to normal breathing data, showing fast recovery from peristalsis and artefacts in the pressure signal.

Resistance scale 1.0 divisions = 1.50 cm H_2O second/litre

Elastance scale 1.0 divisions = 4.605 cm H_2O/litre

Figure 10 Transient response of tracker under panting conditions.

Resistance scale 1.0 divisions = 1.50 cm H_2O second/litre

Elastance scale 1.0 divisions = 4.605 cm H_2O/litre

Figure 11 Tracker response to a change from fast breathing to panting showing a significant increase in elastance.

Resistance scale 1.0 divisions = 1.50 cm H_2O second/litre

Elastance scale 1.0 divisions = 4.605 cm H_2O/litre

R = 0		R = 0.4		R = 0.6		R = 1.0		E
$\hat{E}$	% error	$\hat{E}$	% error	$\hat{E}$	% error	$\hat{E}$	% error	
0.1969	1.55	0.1969	1.55	0.1969	1.55	0.1968	1.60	0.2000
0.2968	1.067	0.2969	1.033	0.2970	1.0	0.2968	1.067	0.3000
0.3966	0.85	0.3968	0.80	0.3966	0.85	0.3971	0.725	0.4000
0.4968	0.64	0.4967	0.66	0.4967	0.66	0.4968	0.64	0.5000
0.5967	0.55	0.5968	0.53	0.5969	0.516	0.5968	0.53	0.6000
0.6967	0.47	0.6967	0.47	0.6968	0.457	0.6968	0.457	0.7000
0.7966	0.425	0.7968	0.40	0.7969	0.387	0.7968	0.40	0.8000
0.8966	0.377	0.8968	0.355	0.8968	0.355	0.8968	0.355	0.9000

TABLE (1) estimated values of the elastance E, for different settings of R using the analogue computer to simulate equation (1). Frequency of sinusoidal signal used = 0.6 Hz, adaptive gain $m_1 = m_2 = 0.8$.

E = 0		E = 0.4		E = 0.6		E = 1.0		R
$\hat{R}$	% error	$\hat{R}$	% error	$\hat{R}$	% error	$\hat{R}$	% error	
0.1972	1.40	0.1972	1.40	0.1972	1.40	0.1974	1.30	0.2000
0.2962	1.27	0.2963	1.233	0.2965	1.16	0.2964	1.20	0.3000
0.3947	1.32	0.3948	1.30	0.3947	1.32	0.3950	1.25	0.4000
0.4937	1.26	0.4937	1.26	0.4938	1.24	0.4939	1.22	0.5000
0.5927	1.21	0.5924	1.26	0.5924	1.26	0.5925	1.25	0.6000
0.6915	1.21	0.6917	1.18	0.6916	1.15	0.6914	1.22	0.7000
0.7917	1.03	0.7917	1.03	0.7914	1.07	0.7912	1.10	0.8000
0.8914	0.95	0.8915	0.944	0.8913	0.966	0.8913	0.966	0.9000

TABLE (2) estimated values of airway resistance R for different settings of E. Frequency of sinusoidal signal used = 0.6 Hz, adaptive gain $m_1 = m_2 = 0.8$.

Adaptive gain settings	Input signal frequency									
	ω=1.0 rad/sec		ω=1.5 rad/sec		ω=1.884 rad/sec		ω=3.768 rad/sec		ω=6.28 rad/sec	
	convergence time in seconds		convergence time in seconds		convergence time in seconds		convergence time in seconds		convergence time in seconds	
$m_1=m_2$	t_R	t_E	t_R	t_E	t_R	t_E	t_R	t_E	t_R	t_E
0.1	10.4	9.0	8.75	8.70	9.40	10.2	9.95	11.30	10.38	10.60
0.2	6.10	5.55	4.88	4.45	6.44	5.20	4.60	5.10	5.28	5.28
0.3	3.85	3.40	3.10	2.88	4.11	3.33	3.15	3.50	3.77	3.60
0.4	1.57	0.95	2.85	2.27	2.78	2.08	2.25	2.60	2.82	2.62
0.5	1.40	0.85	1.18	0.80	2.68	1.95	2.12	1.90	2.33	2.00
0.6	6.88	5.65	0.88	0.73	2.40	1.55	2.08	1.80	2.25	1.80
0.7	7.15	6.20	1.05	1.55	2.20	1.40	1.43	1.53	1.78	1.62
0.8	10.33	8.75	2.55	2.10	0.89	0.55	1.42	1.05	1.70	1.26
0.9	13.22	12.00	4.75	4.18	2.12	2.15	1.40	1.00	1.35	1.10
1.0	19.40	17.40	4.90	4.80	4.00	2.43	1.18	0.90	1.15	1.00

TABLE (3) Variation of the convergence time of the parameters R and E to settle within 5% of its steady-state value with the adaptive gain settings measured at frequencies 1.0, 1.5, 1.884, 3.768 and 6.28 rad/sec.

Breathing frequency (Hz)	Elastance E_s (Volt)	E (cm H_2O/l)	Resistance R_s (Volt)	R (cm H_2O sec./l)	Notes
0.26	2.0	7.37	4.00	4.80	one cycle after peristalsis wave
0.30	1.50	5.53	2.40	2.88	
0.40	1.80	6.63	3.60	4.32	one cycle after artefact in pressure signal
0.50	1.90	7.00	2.62	3.14	
0.59	2.25	8.30	2.65	3.18	
1.11	3.75	13.82	3.00	3.6	

TABLE (4) change of lung parameters with the

frequency of breathing.

time as indicated in figures	loop slope (1)	loop slope (2)	loop slope (3)	loop slope (4)	loop slope (5)	average slope	standard deviation	R loop-flatt. ($cmH_2Osec/1$)	R-track ($cmH_2Osec/1$)	E-track ($cmH_2O/1$)
$t = t_1$	1.50	1.56	1.33	1.60	1.31	1.46	0.118	1.82	2.40	4.80
$t = t_2$	1.47	1.70	1.45	1.50	1.50	1.52	0.098	1.90	2.72	5.50
$t = t_3$	1.67	1.54	1.62	1.54	1.56	1.58	0.0515	1.98	2.76	5.53

TABLE (5) Estimation of airway resistance and lung elastance at three different stretches of normal breathing using both loop-flattening technique and adaptive tracker.

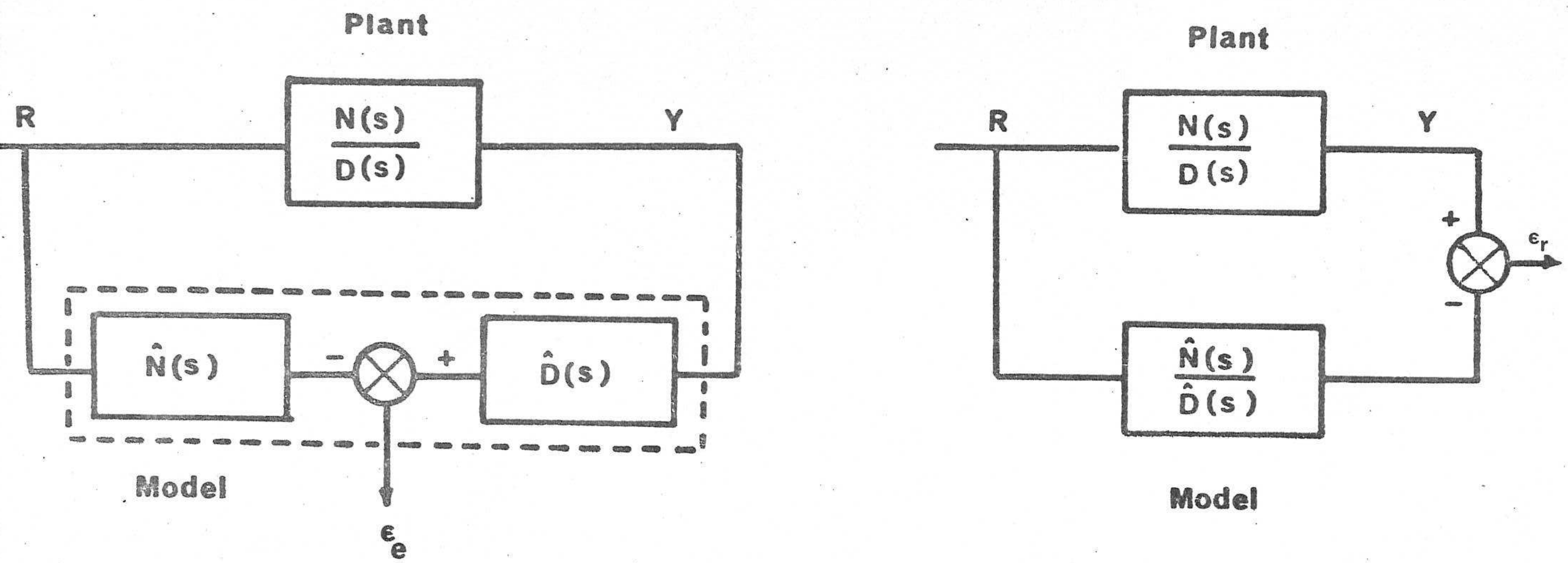

Equation Error System

Response Error System

Fig (1)

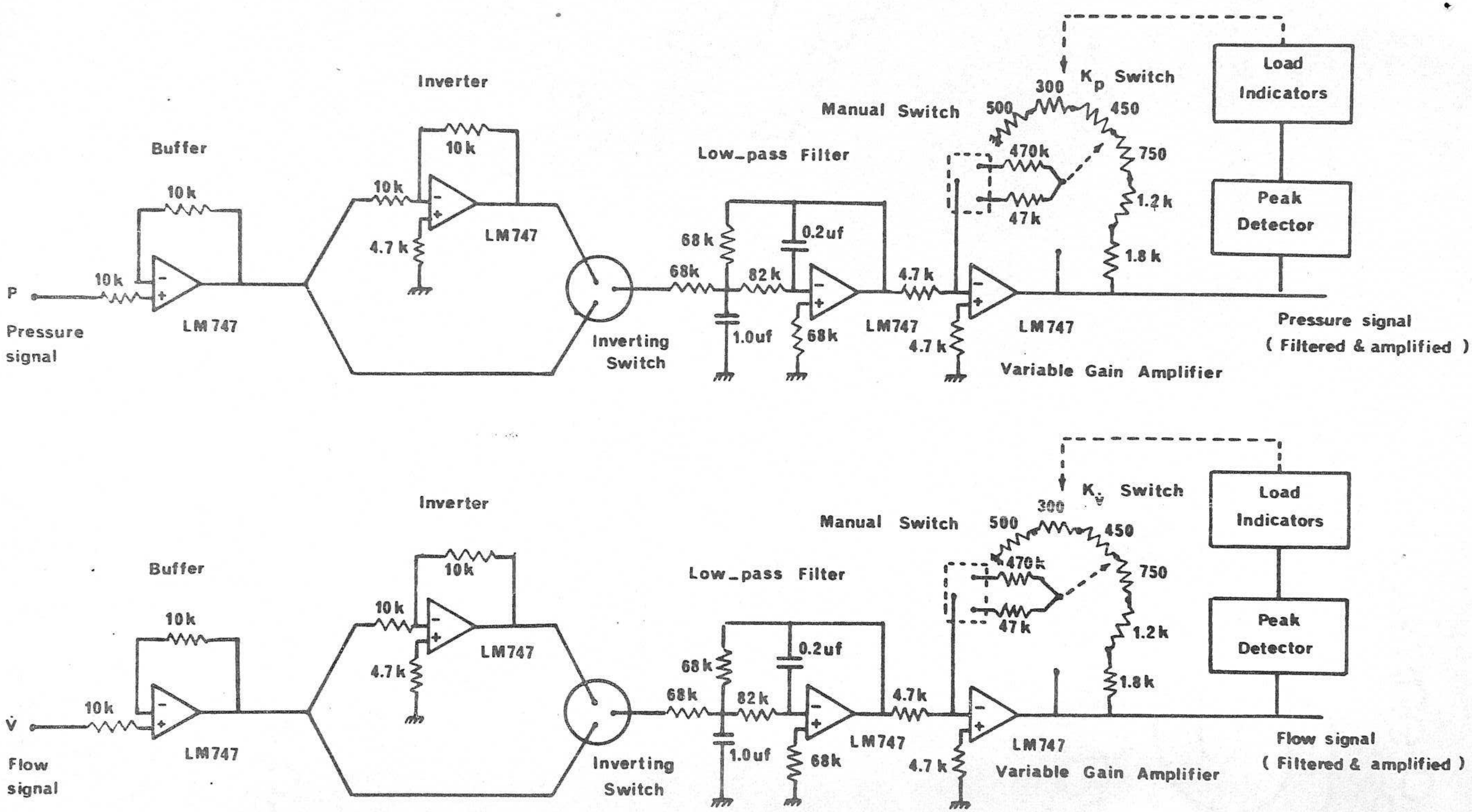
Buffer
10k
10k
LM747
P
Pressure signal
Inverter
10k
10k
4.7k
LM747
Inverting Switch
Low_pass Filter
68k
68k
82k
0.2uf
1.0uf
68k
LM747
4.7k
4.7k
Manual Switch
500
300
K_p Switch
450
750
1.2k
1.8k
470k
47k
LM747
Variable Gain Amplifier
Load Indicators
Peak Detector
Pressure signal
(Filtered & amplified)
Buffer
10k
10k
LM747
$\dot{V}$
Flow signal
Inverter
10k
10k
4.7k
LM747
Inverting Switch
Low_pass Filter
68k
68k
82k
0.2uf
1.0uf
68k
LM747
4.7k
4.7k
Manual Switch
500
300
$K_{\dot{V}}$ Switch
450
750
1.2k
1.8k
470k
47k
LM747
Variable Gain Amplifier
Load Indicators
Peak Detector
Flow signal
(Filtered & amplified)

Fig(2)

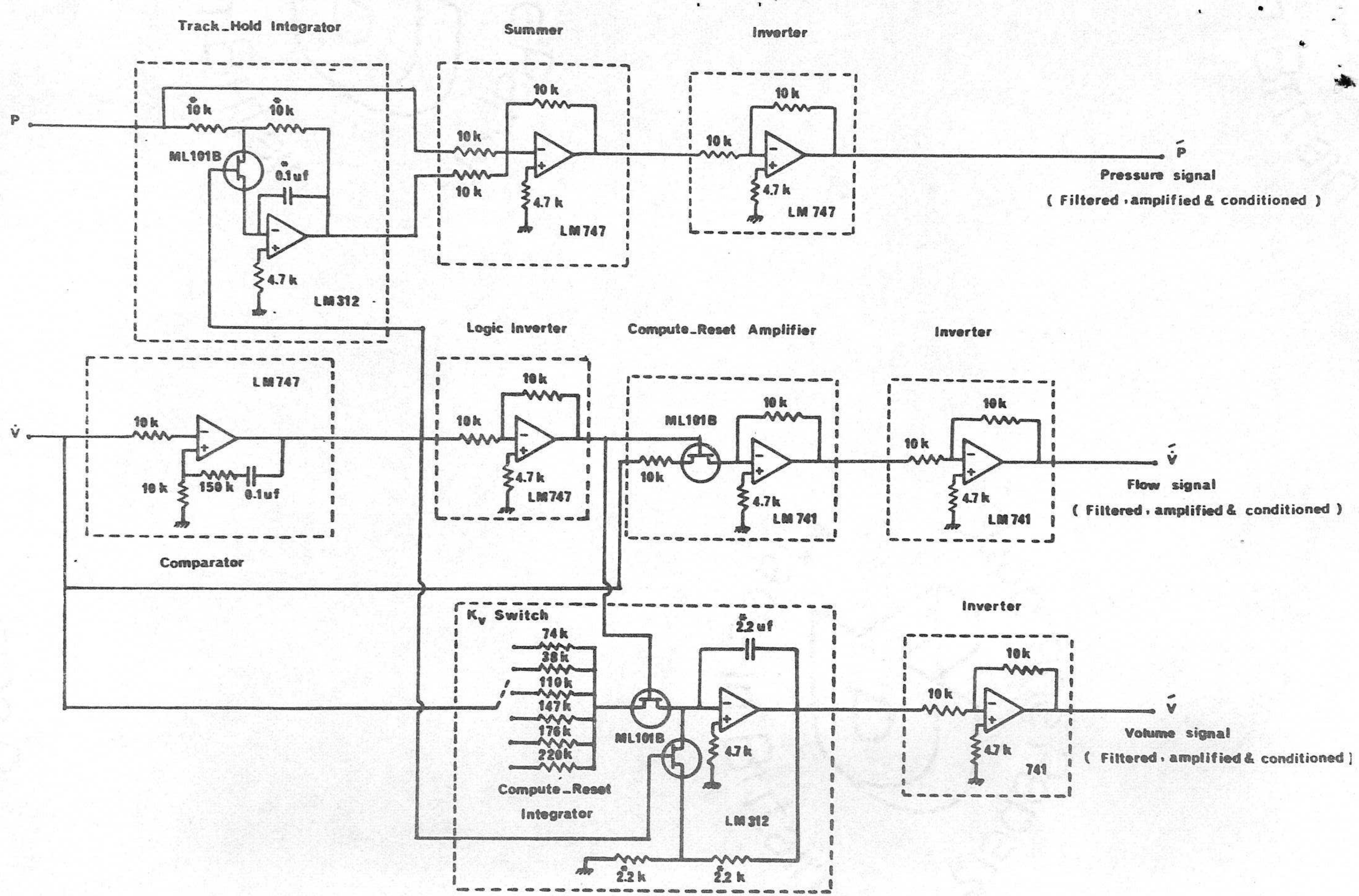
Track_Hold Integrator
Summer
Inverter
10 k
10 k
ML101B
0.1uf
4.7 k
LM 312
LM 747
Pressure signal
(Filtered , amplified & conditioned)
Logic Inverter
Compute_Reset Amplifier
LM 747
150 k
0.1uf
Comparator
LM 741
Flow signal
(Filtered , amplified & conditioned)
Kv Switch
74k
38k
110k
147k
176k
220k
2.2 uf
Compute_Reset
Integrator
2.2 k
741
Volume signal
(Filtered , amplified & conditioned)

Fig (3)

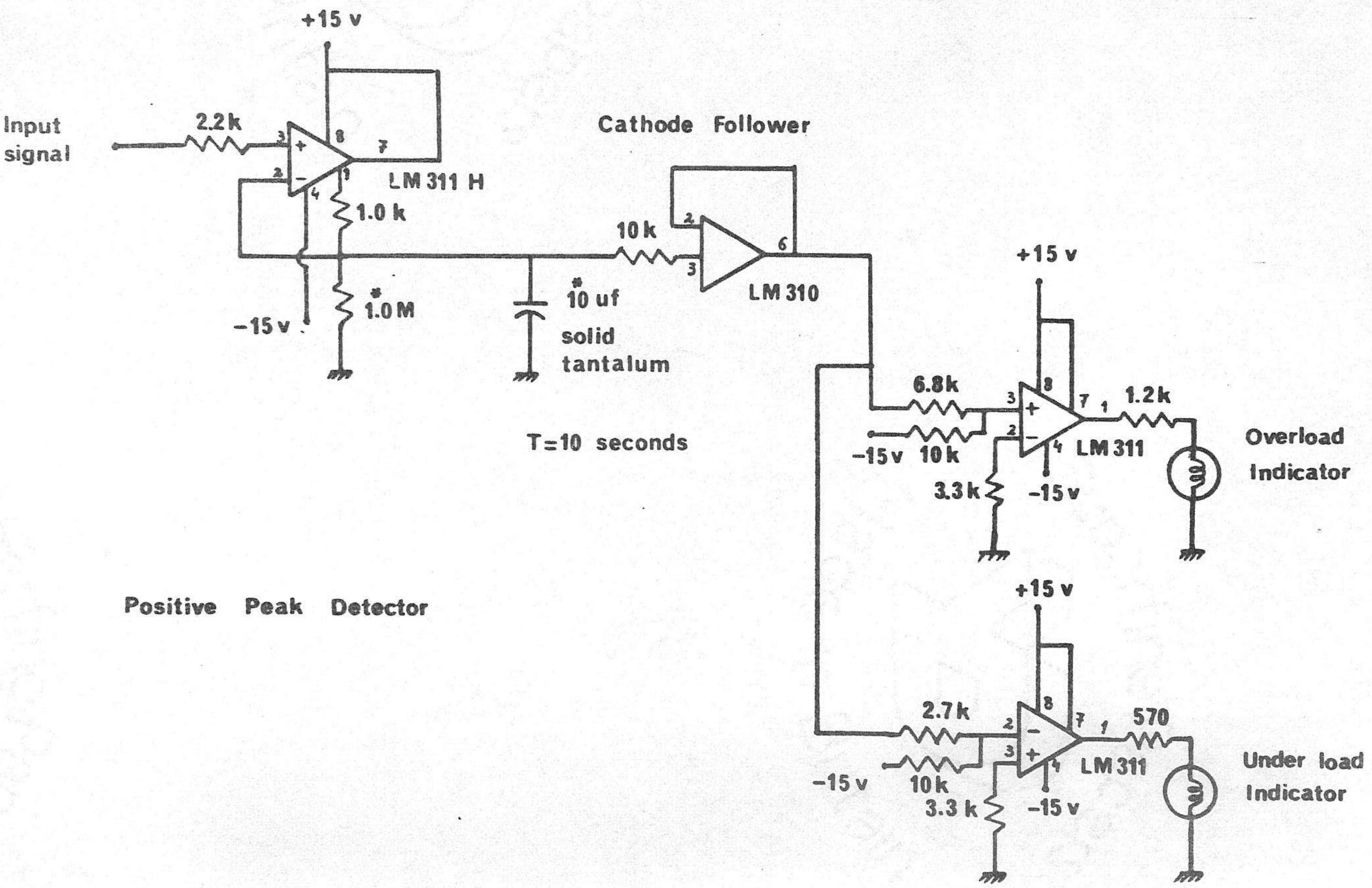
Input
signal
2.2k
+15 v
LM 311 H
1.0 k
-15 v
* 1.0 M
Cathode Follower
10 k
LM 310
* 10 uf
solid
tantalum
T=10 seconds
Positive Peak Detector
+15 v
6.8k
-15 v 10 k
3.3 k
LM 311
-15 v
1.2 k
Overload
Indicator
+15 v
2.7 k
-15 v
10 k
3.3 k
LM 311
-15 v
570
Under load
Indicator

Fig(4)

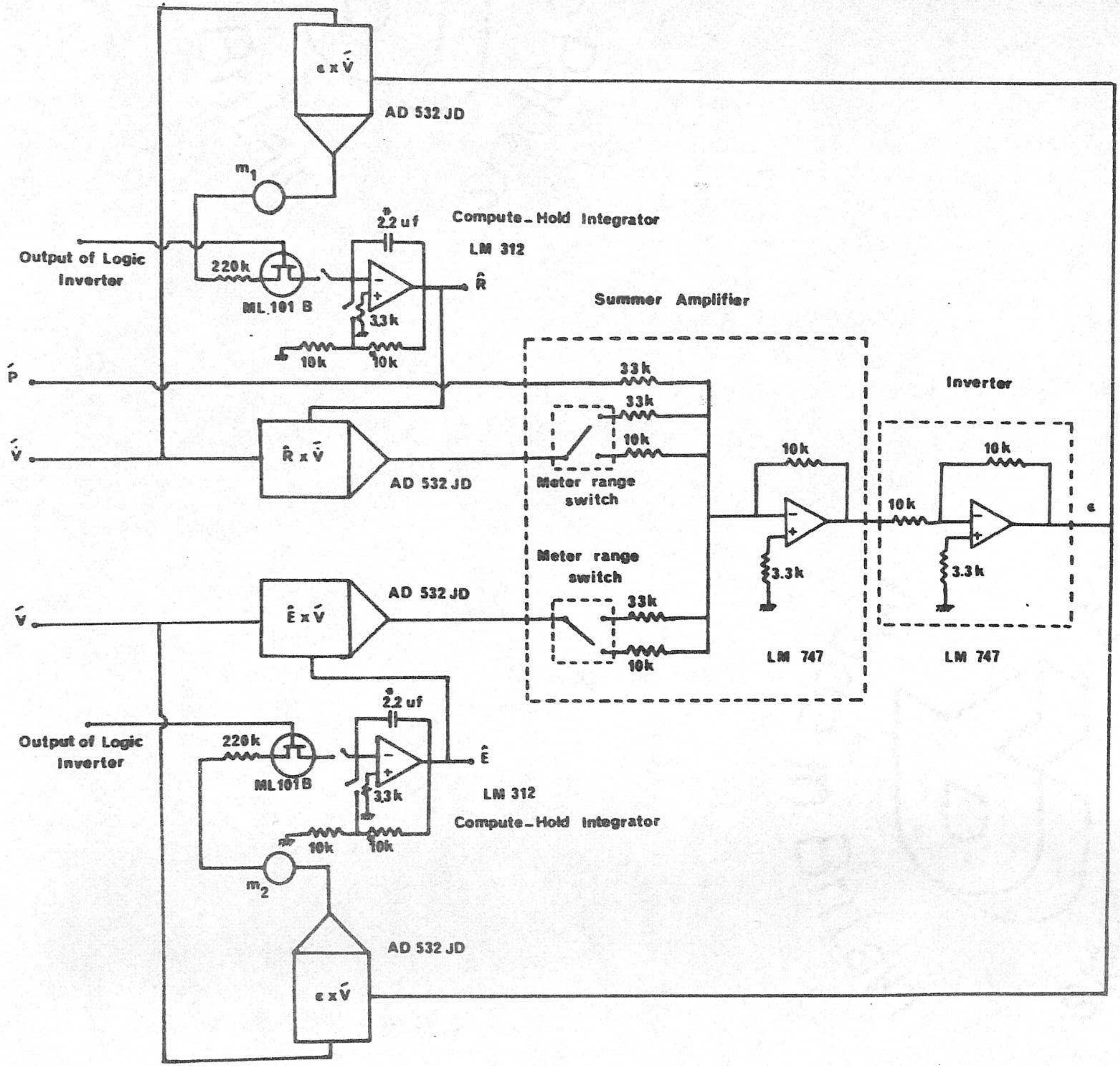

ε x V́
AD 532 JD
m1
2.2 uf
Compute_Hold Integrator
LM 312
Output of Logic Inverter
220k
ML 101 B
R̂
3.3k
10k
10k
Summer Amplifier
Ṕ
V́
R̂ x V́
AD 532 JD
33k
33k
10k
Meter range switch
Inverter
10k
10k
10k
ε
Meter range switch
3.3k
3.3k
Ê x V́
AD 532 JD
33k
10k
LM 747
LM 747
2.2 uf
Output of Logic Inverter
220k
ML101B
Ê
3.3k
LM 312
Compute_Hold Integrator
10k
10k
m2
AD 532 JD
ε x V́

Fig(5)

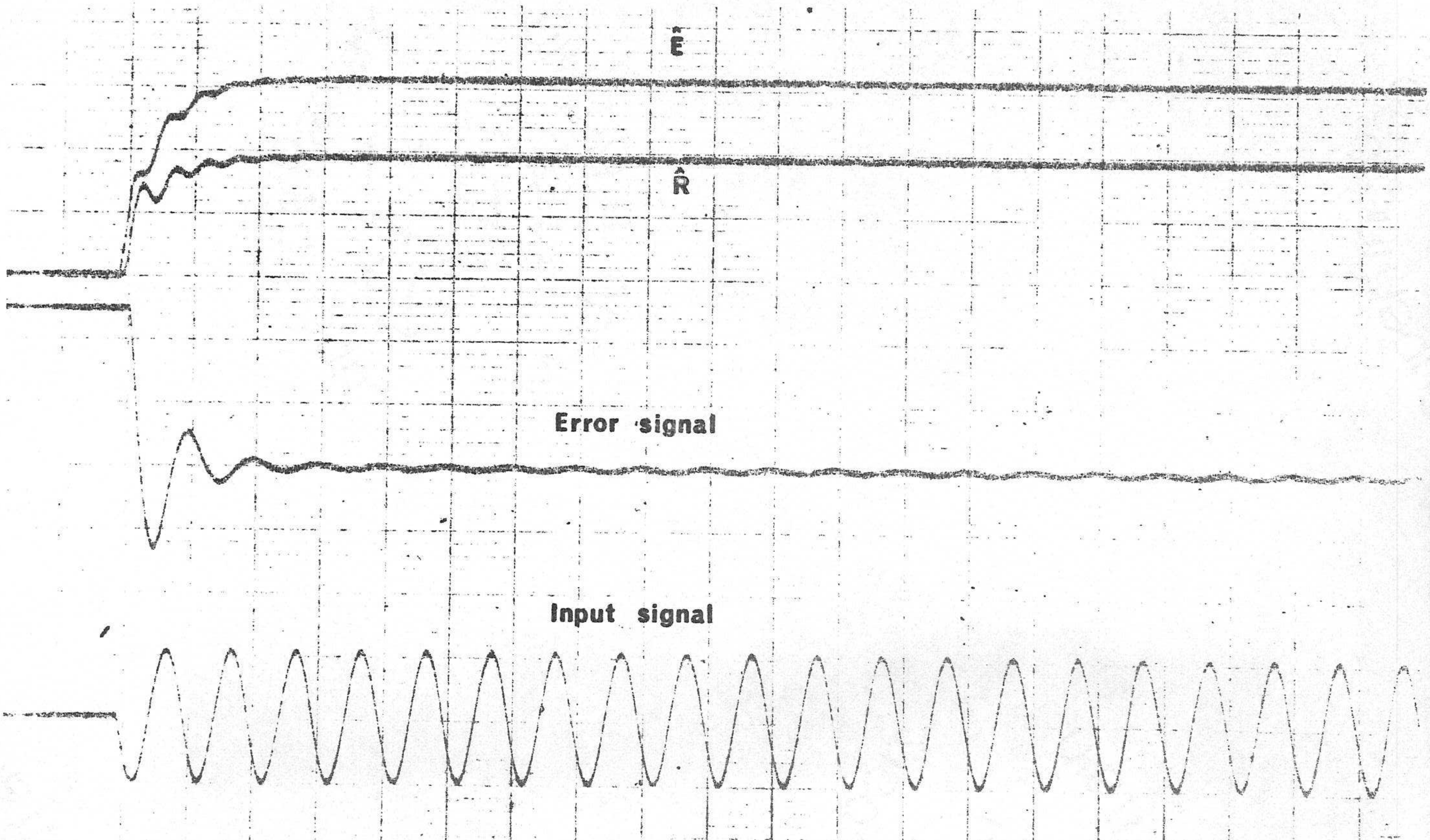

Fig (6) a

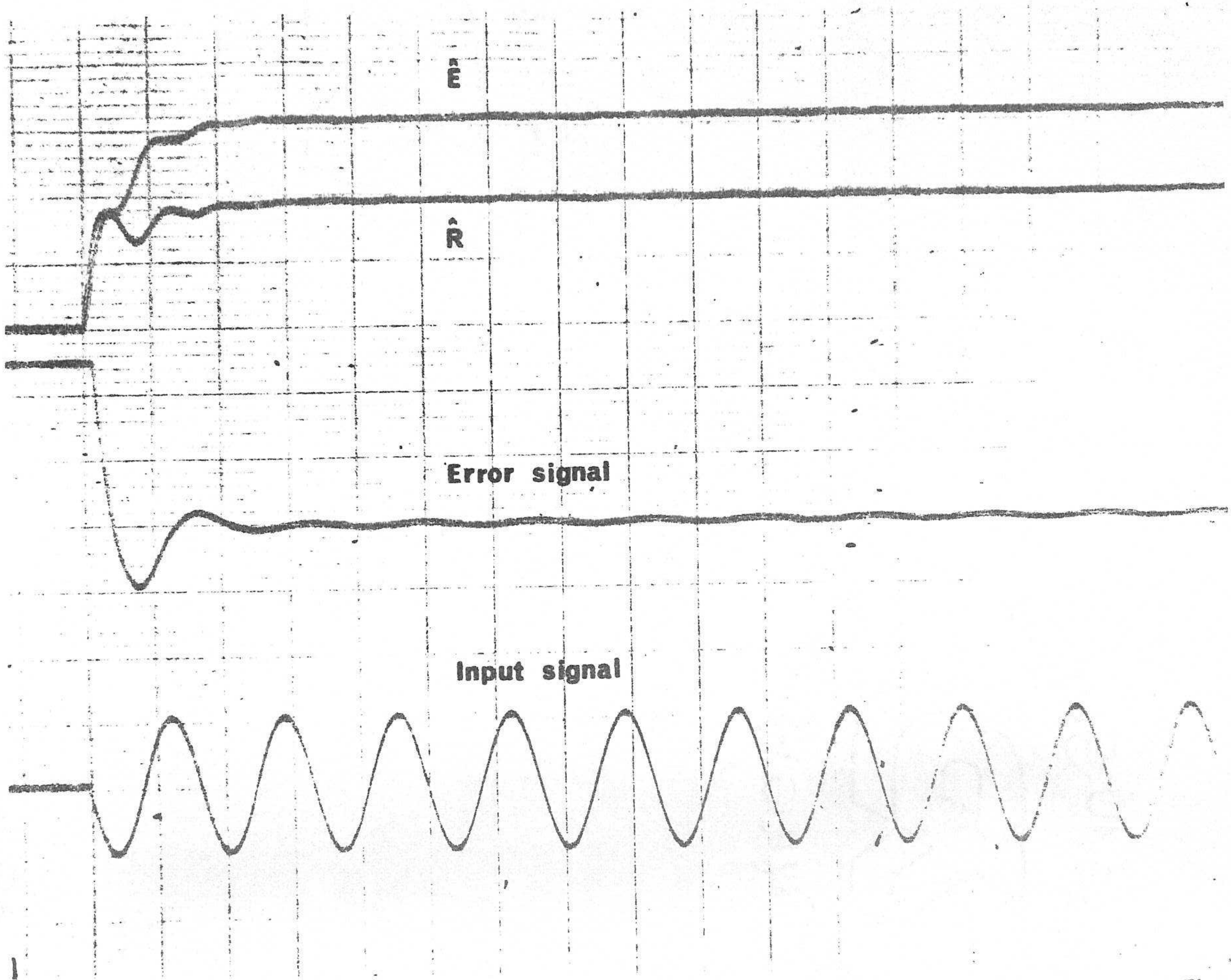

Fig (6) b

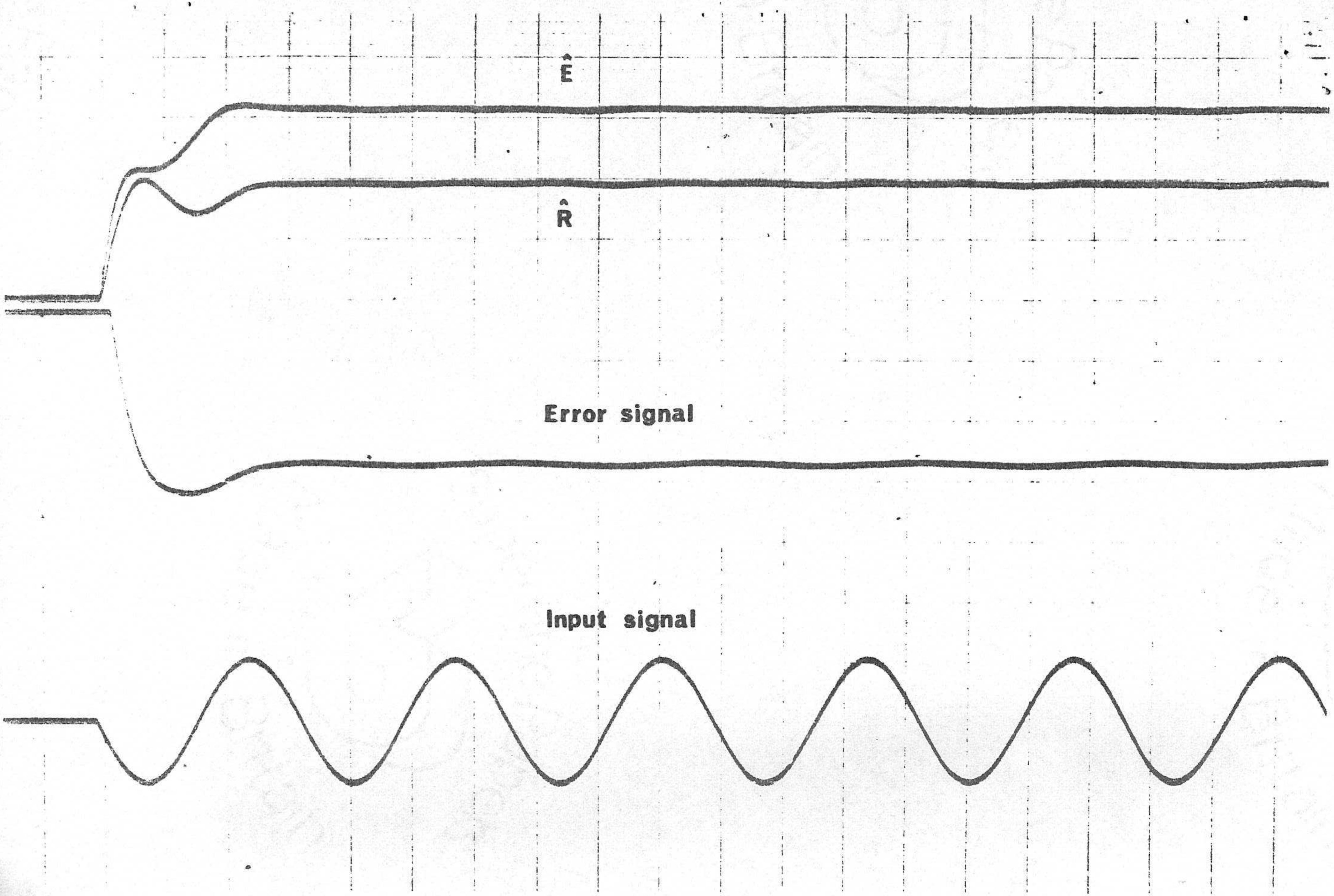

Fig(6)c

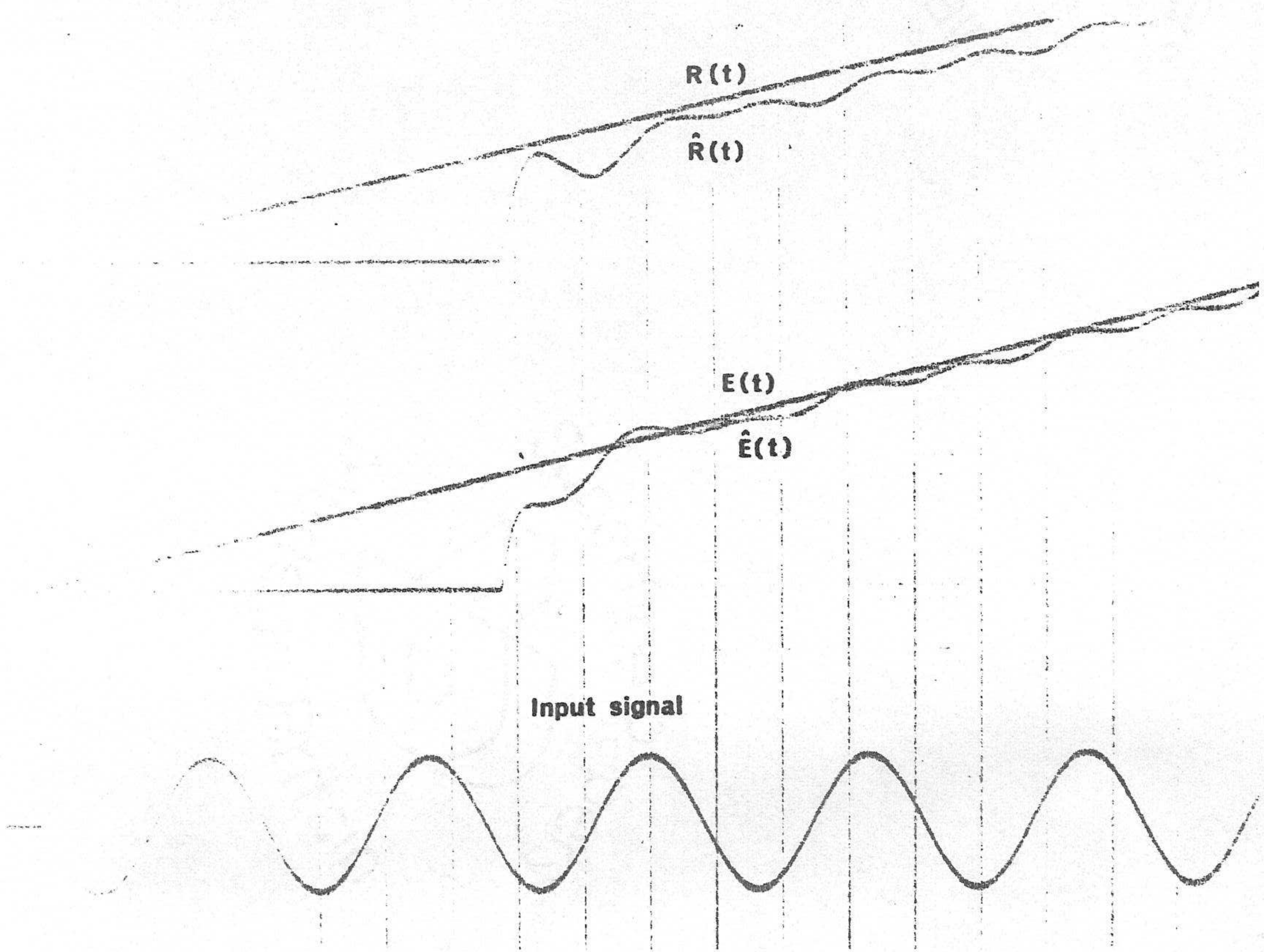

Fig(7)a

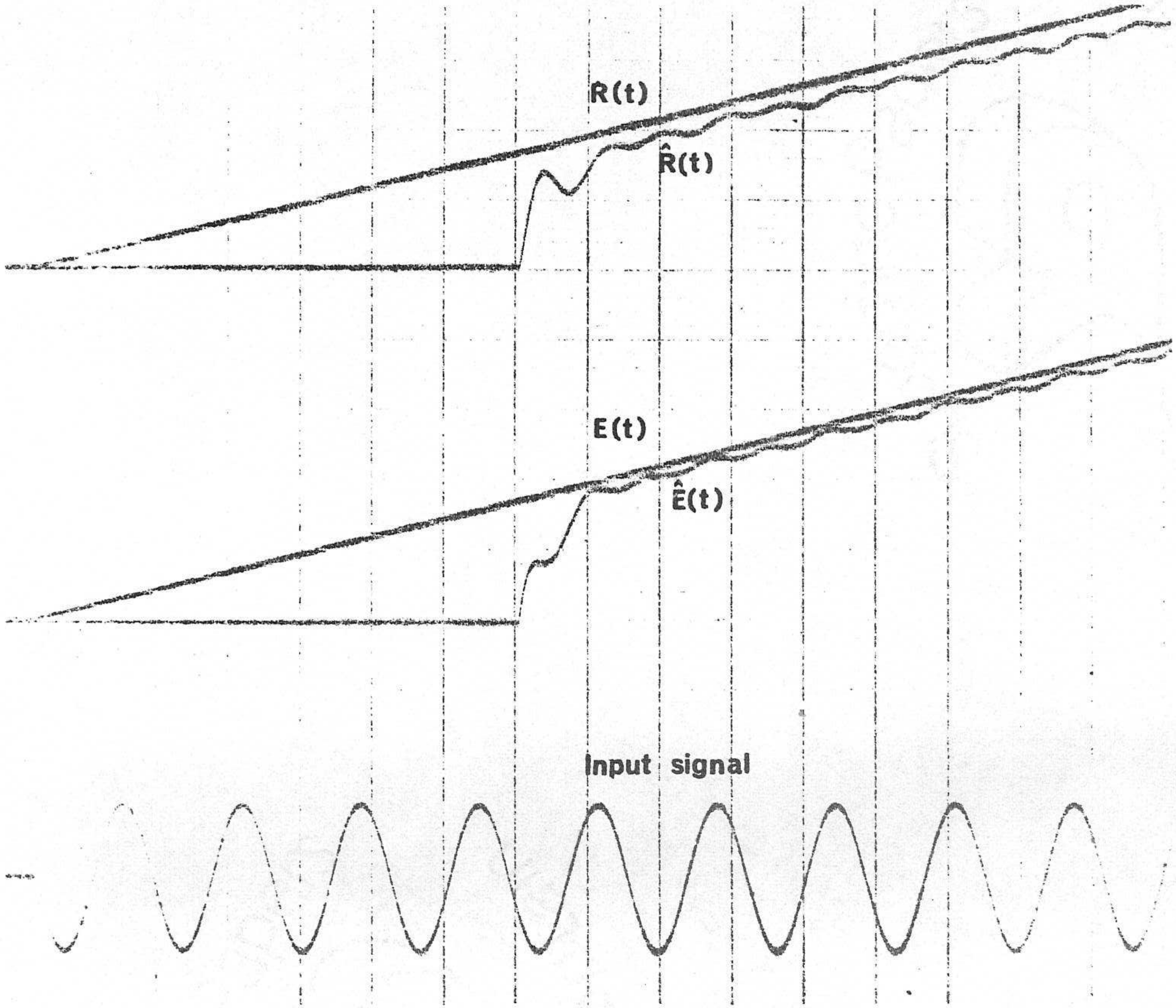

Fig(7)b

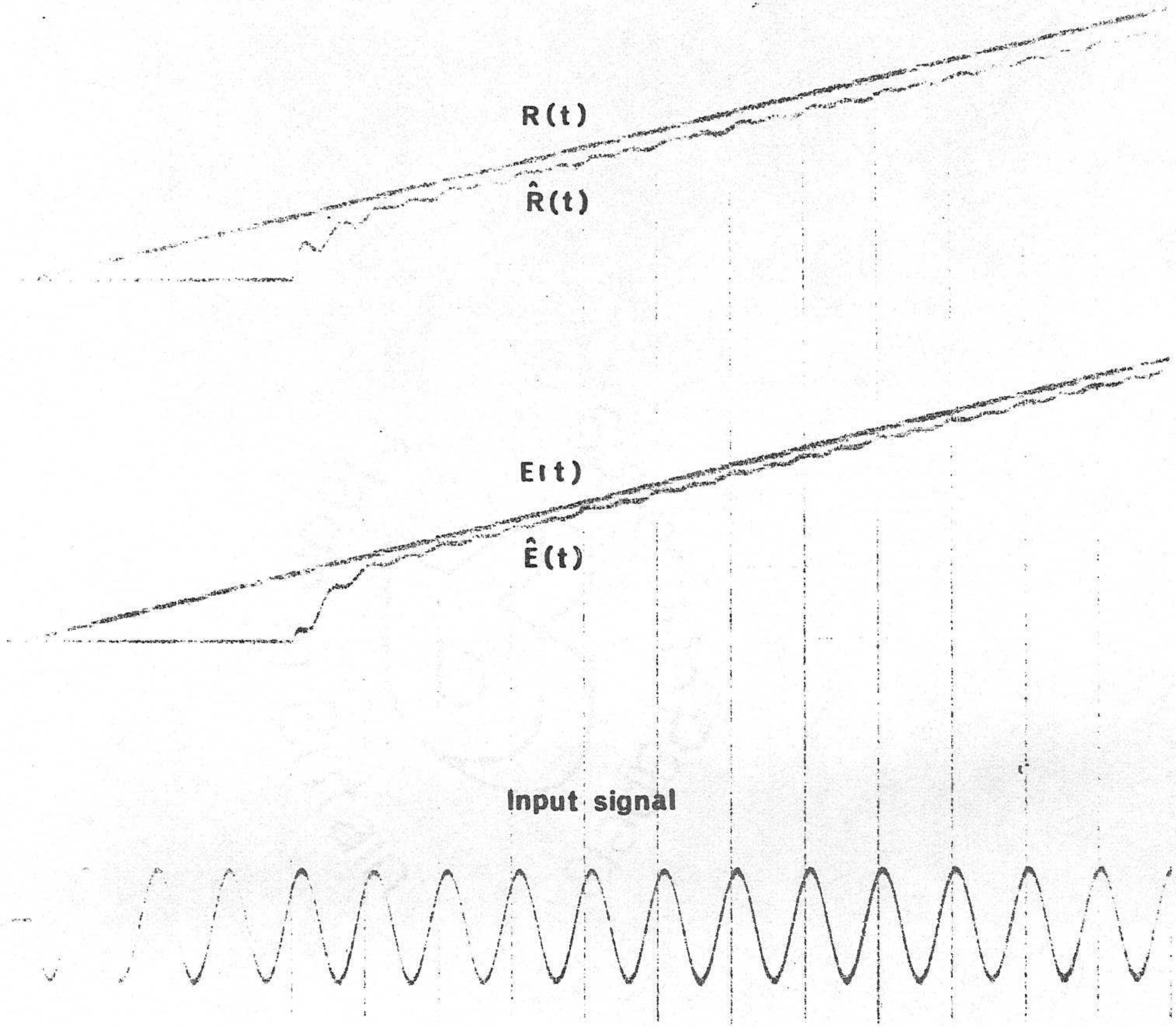

Fig(7)c

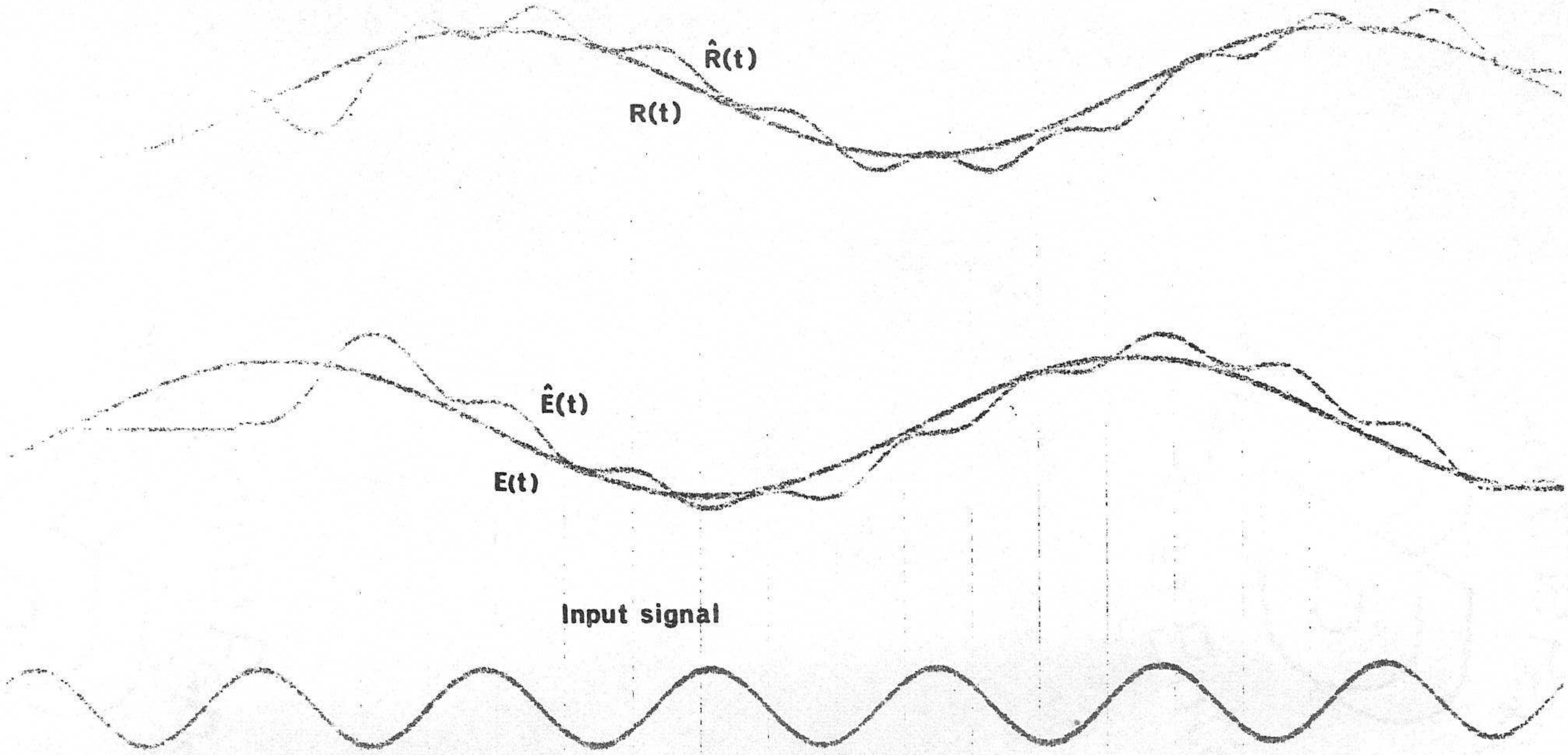

Fig(8)a

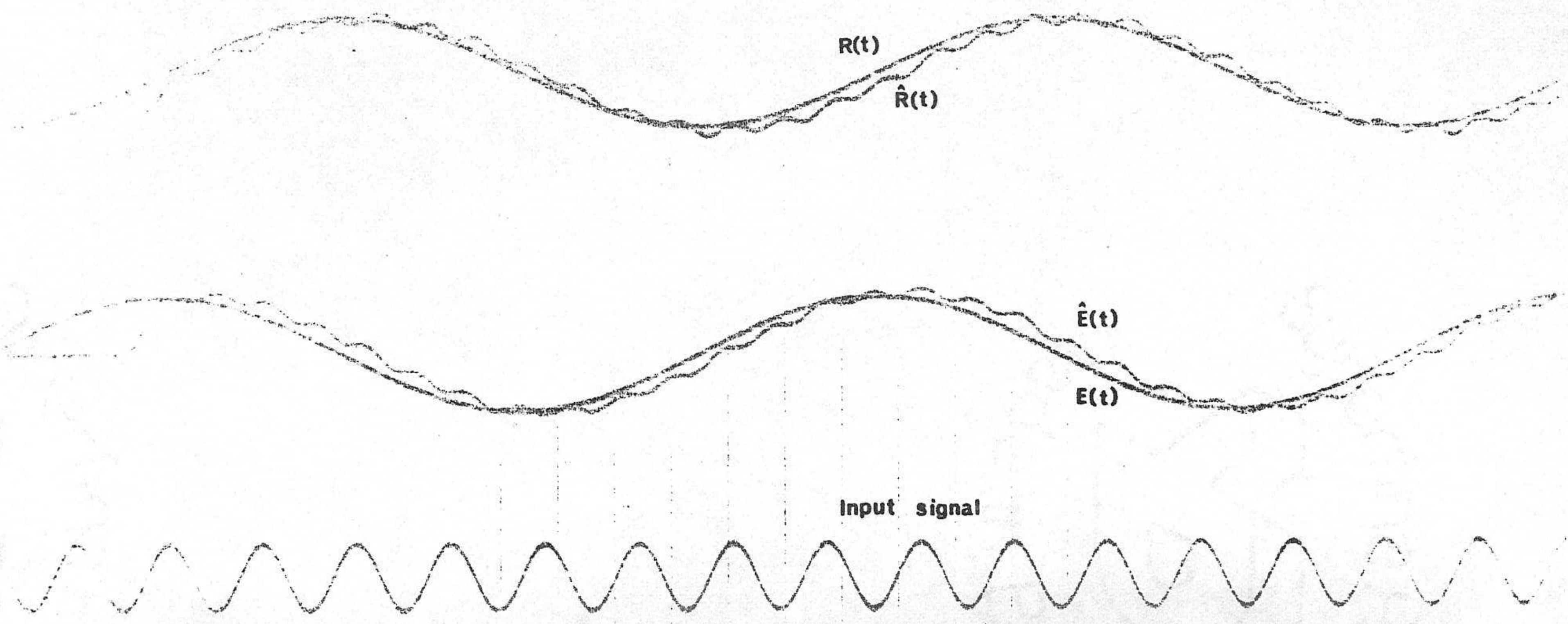

Fig(8)b

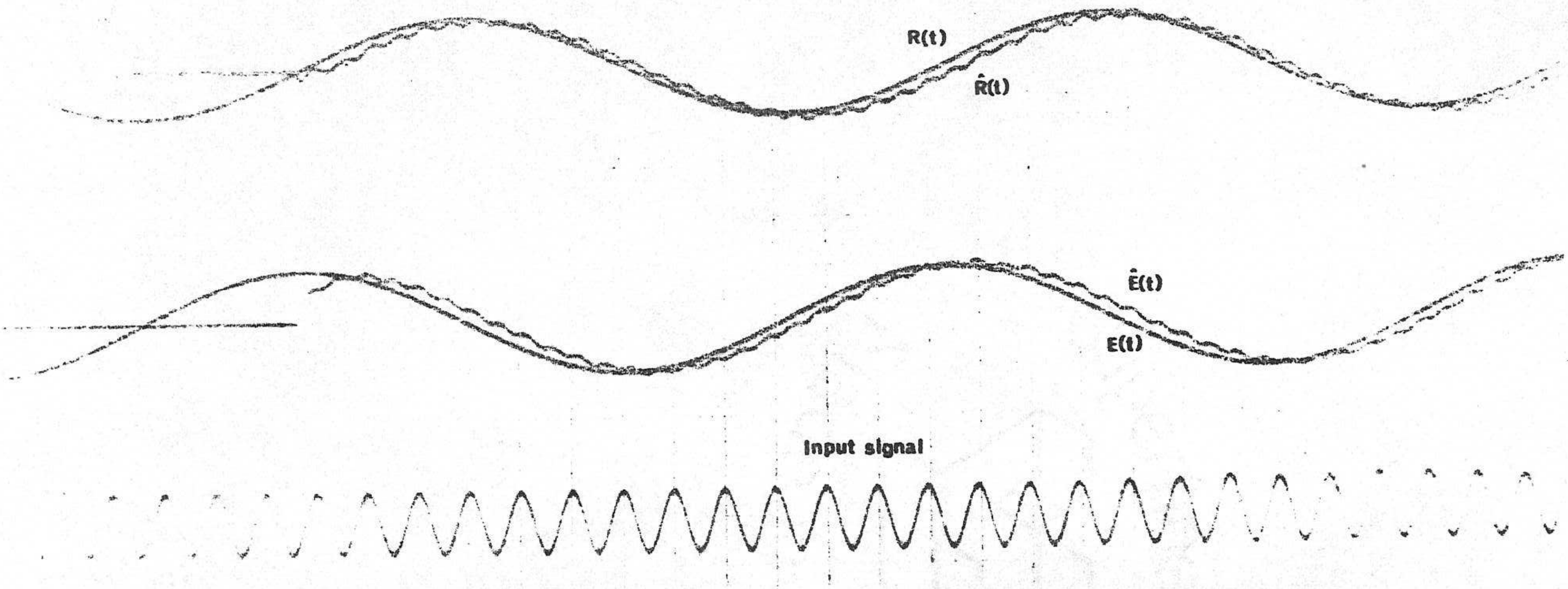

Fig (8)c

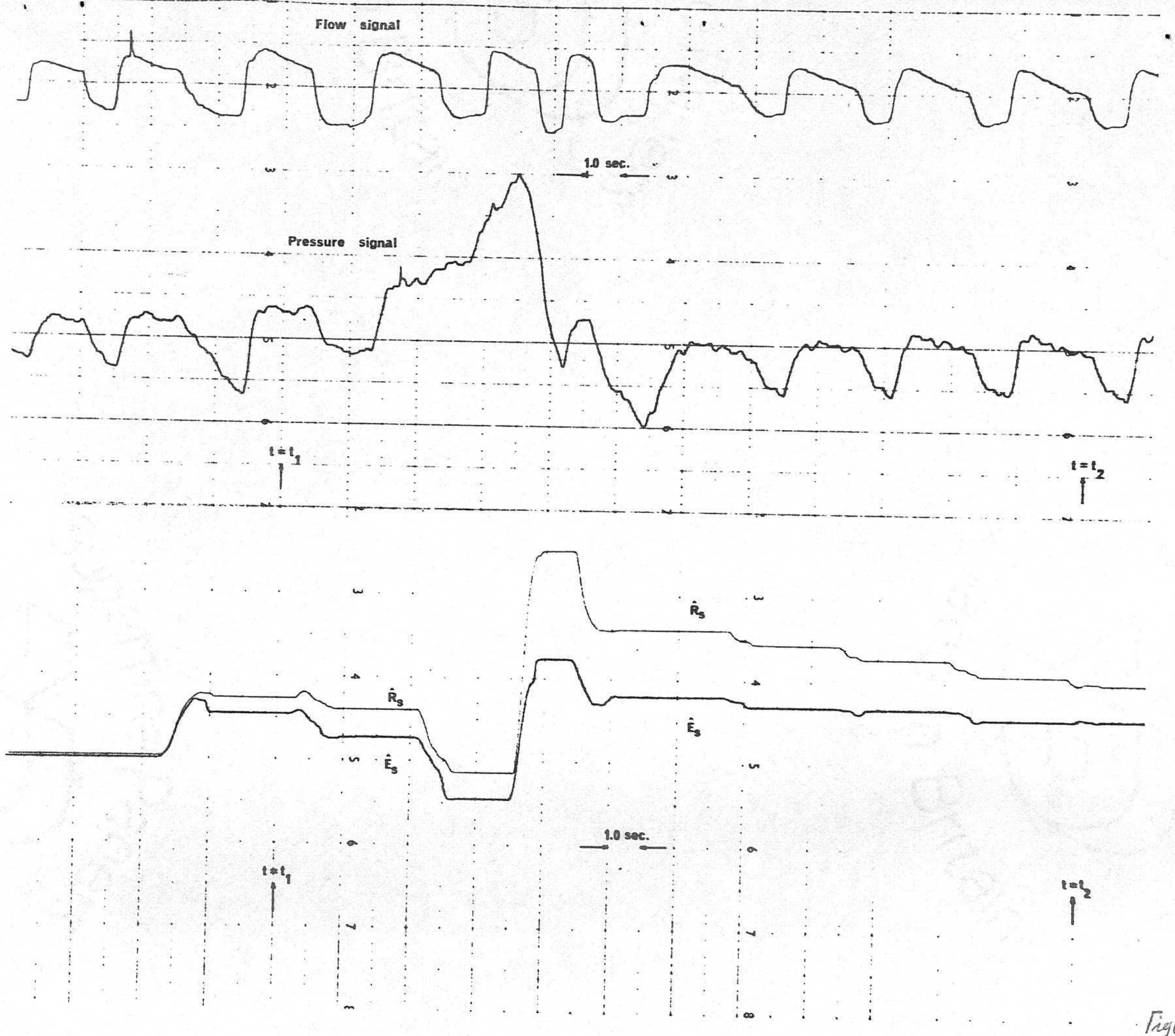

Flow signal
1.0 sec.
Pressure signal
t = t1
t = t2
R̂s
Ês
1.0 sec.
t = t1
t = t2

Fig(9)a

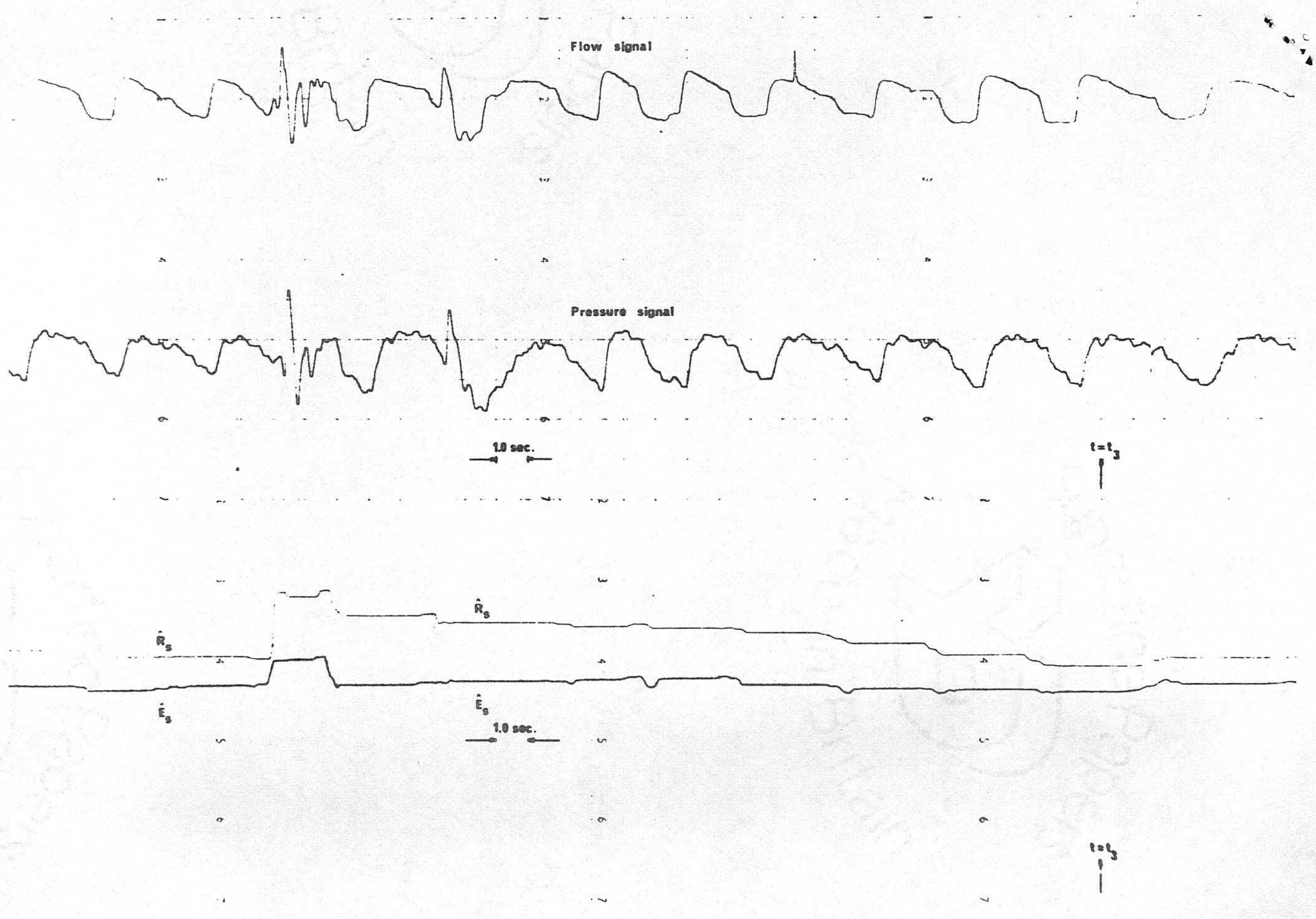

Fig(9)b

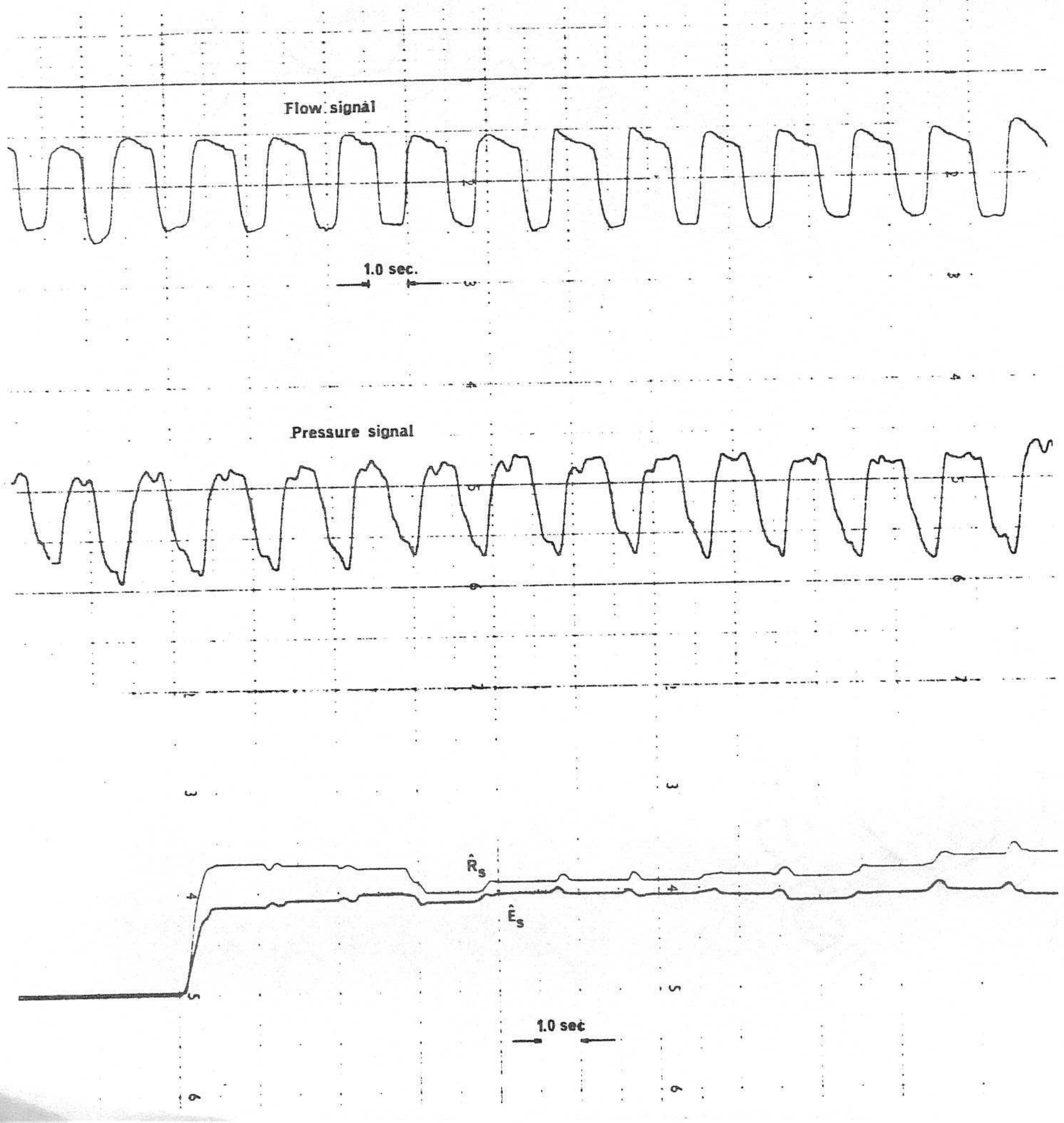

Fig(10)